

**Biophysical Journal, Volume 99**

**Supporting Material**

**Electrostatic Interactions and Binding Orientation of HIV-1 Matrix, Studied by Neutron Reflectivity**

*Hirsh Nanda, Siddhartha A. K. Datta, Frank Heinrich, Mathias Lösche, Alan Rein, Susan Krueger, Joseph E. Curtis*

## Supporting Material:

### Electrostatic Interactions and Binding Orientation of HIV-1 Matrix, Studied by Neutron Reflectivity

*Hirsh Nanda, Siddhartha A. K. Datta, Frank Heinrich, Mathias Lösche, Alan Rein, Susan Krueger, Joseph E. Curtis*

#### Protein Purification (1).

Columns used for protein purification were from GE Health Care Life Sciences. The HIV MA protein was expressed using a PET 3XC vector in BL21 (DE3) pLysS cells. The cells expressing HIV MA were induced at 37° C for 4 hours with 1 mM isopropyl  $\beta$ -D-1-thiogalactopyranoside (IPTG), and lysed in buffer A (20 mM Tris HCl, pH 7.4, 10 mM  $\beta$ -ME and 1 mM phenylmethylsulphonyl fluoride (PMSF)) with 150 mM NaCl. After centrifugation at 12,000 g for 15 min to remove cellular debris, HIV MA protein was fractionated from the lysate by taking a 40-70% ammonium sulfate saturation cut. The protein was dialyzed against buffer A with 150 mM NaCl. Ammonium sulfate was added to 40% saturation and the solution was chromatographed on a butyl Sepharose column. Fractions containing the protein were dialyzed against buffer A with 50 mM NaCl, and chromatographed on an SP Sepharose column. The purified protein was stored in buffer A with 150 mM NaCl and 10% glycerol, and chromatographed on a Superdex 75 gel filtration column before experiments.

#### Modeling Electrostatic Interactions with the Gouy-Chapman Double Layer Model

A simplified theoretical model describing the electrostatic potential due to a charged membrane is provided by the Gouy-Chapman theory of the double electric layer (2). The membrane is represented as a plane where discrete charges from the anionic lipids are replaced by an averaged surface charge density. The theory provides a specific solution to the 1-D Poisson-Boltzmann equation for the planar geometry. The electrostatic potential at a distance,  $z$ , from the membrane surface is given by

$$\Phi(z) = \Phi_0 e^{-\kappa z} \quad (2),$$

where  $\Phi_0$  is the surface potential (at  $z = 0$ ) and  $1/\kappa$  is the Debye screening length. The surface potential is provided by the equation

$$\Phi_0 = \frac{0.0514}{Z} \sinh^{-1} \left[ \frac{136.6\sigma}{\sqrt{C}} \right] \quad (3)$$

for  $T = 298$  K for a 1:1 ion valence electrolyte.  $Z$  is the absolute valence of the electrolyte,  $\sigma$  is the surface charge density in  $e^-/\text{\AA}^2$ , and  $C$  is the concentration of electrolyte in mol/L.  $\Phi_0$  is in units of volts.

The electrostatic energy as a function of protein orientation was calculated by applying the same rigid body rotations to the NMR structure of MA as described for reflectivity

fitting. The partial charge for each atom of MA was assigned using the CHARMM22 force field (3). For each protein orientation, the total electrostatic energy,  $E$ , was computed as

$$E = \sum_{i=1}^N dQ_i \Phi(z_i) \quad (4)$$

where  $dQ_i$  is the partial charge of atom  $i$  and  $z_i$  is the distance of that atom from the membrane surface, as determined by the protein orientation. The sum is over all  $N$  atoms of the MA protein. This application of Gouy-Chapman theory is deemed sufficient for a first approximation of electrostatic interactions as a function of MA orientation. Application of the full Poisson-Boltzmann equation and atomistic representations of membranes have been reported elsewhere (4-6).

## Figures

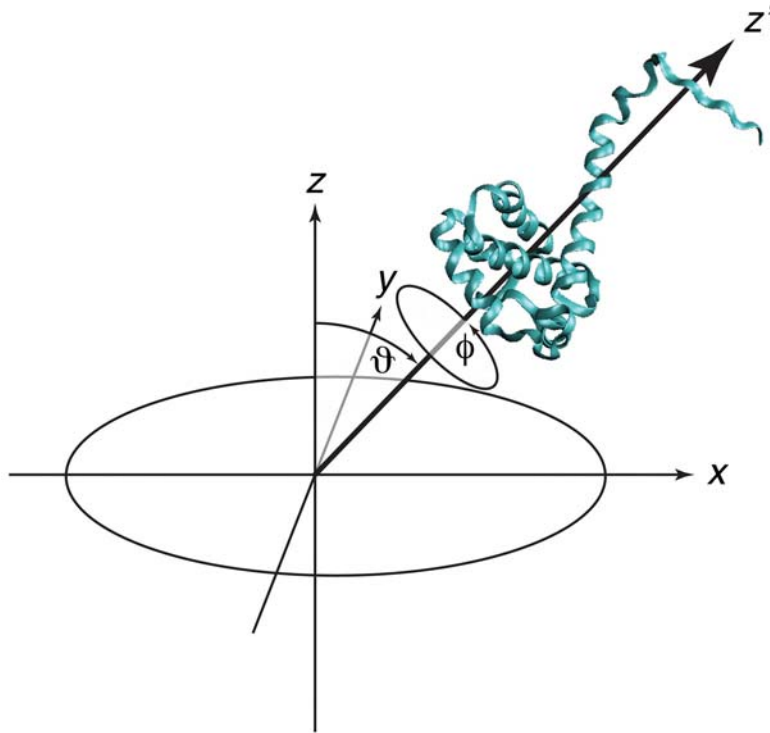


**Figure S1.** Two Euler angles,  $\vartheta$  and  $\phi$ , are used to define the orientation of the protein at the membrane surface. Further description of the polar rotation angles is provided in the Materials and Methods section of the main text.

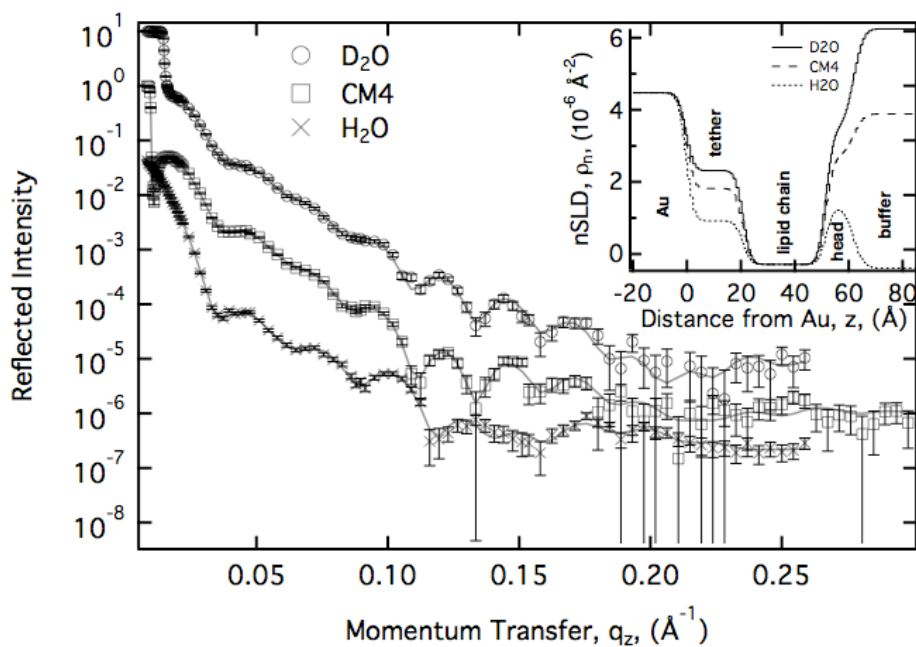
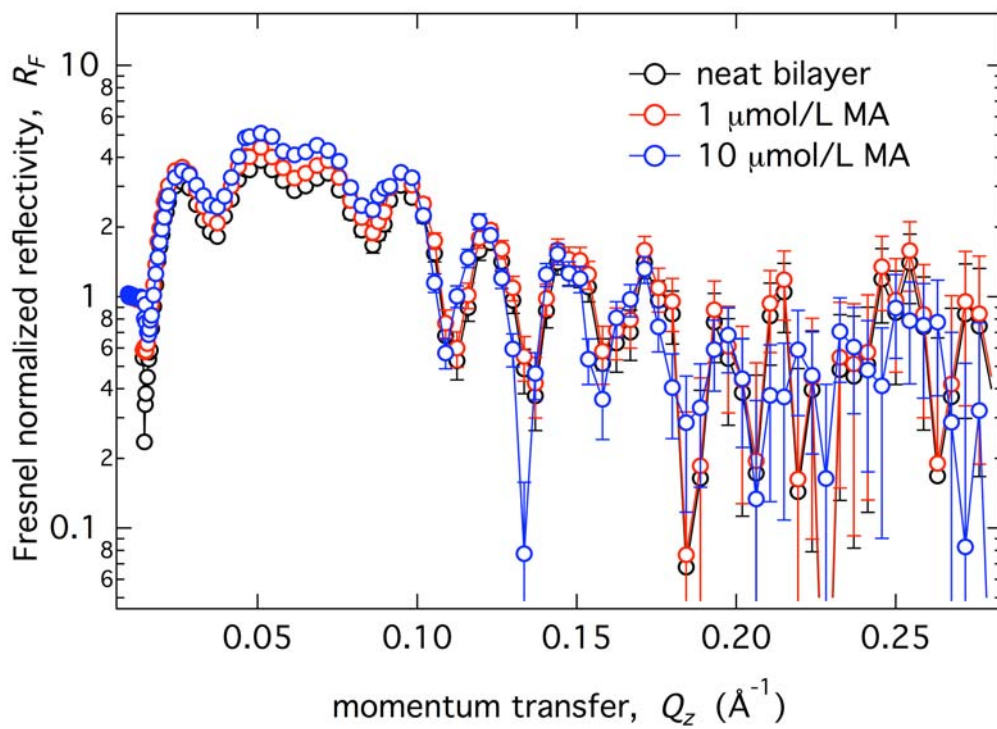
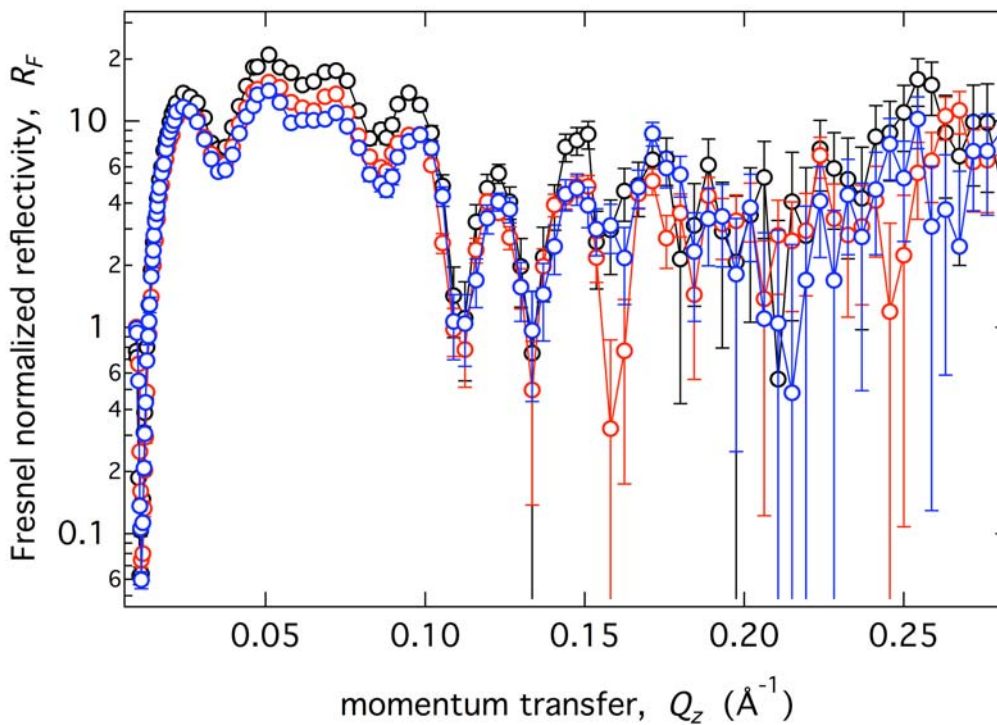


**Figure S2.** Neutron reflectivities of a neat tBLM composed of 70% DMPC/30% DMPS with  $\sim 3$  mol% cholesterol in three isotopically distinct buffers:  $D_2O$ ,  $D_2O:H_2O$  2:1 (CM4), and  $H_2O$ . Simultaneous fits of a box model to all three isotopic solvent contrasts are shown (solid line). The resulting SLD profiles for the three contrasts are provided in the inset. The fact that the SLDs of the lipid chain region in each contrast are identical indicates complete ( $> 99\%$ ) surface coverage of the bilayer on the substrate surface.

a)



b)



c)

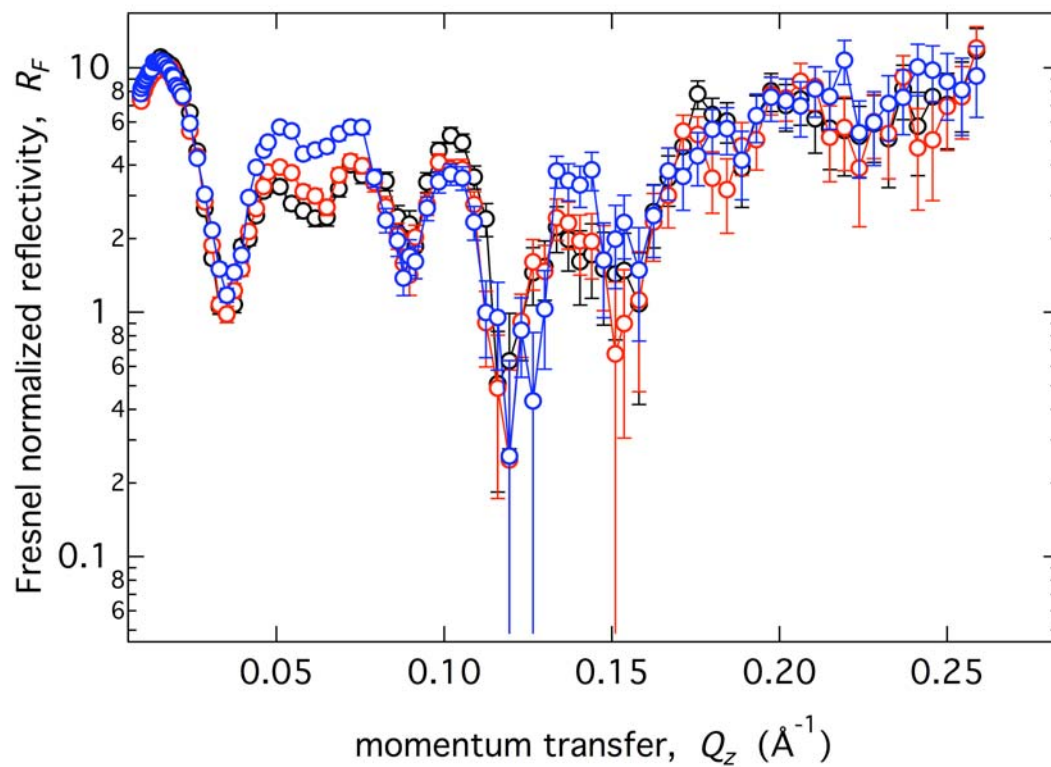


**Figure S3:** Reflectivity data sets for MA binding to the tBLM characterized in Fig. S2. Each panel shows a different isotopic solvent composition. a) D<sub>2</sub>O buffer, b) CM4 buffer, c) H<sub>2</sub>O buffer under different protein binding conditions: pure bilayer (black), 1 μmol/L MA (red) and 10 μmol/L MA (blue).

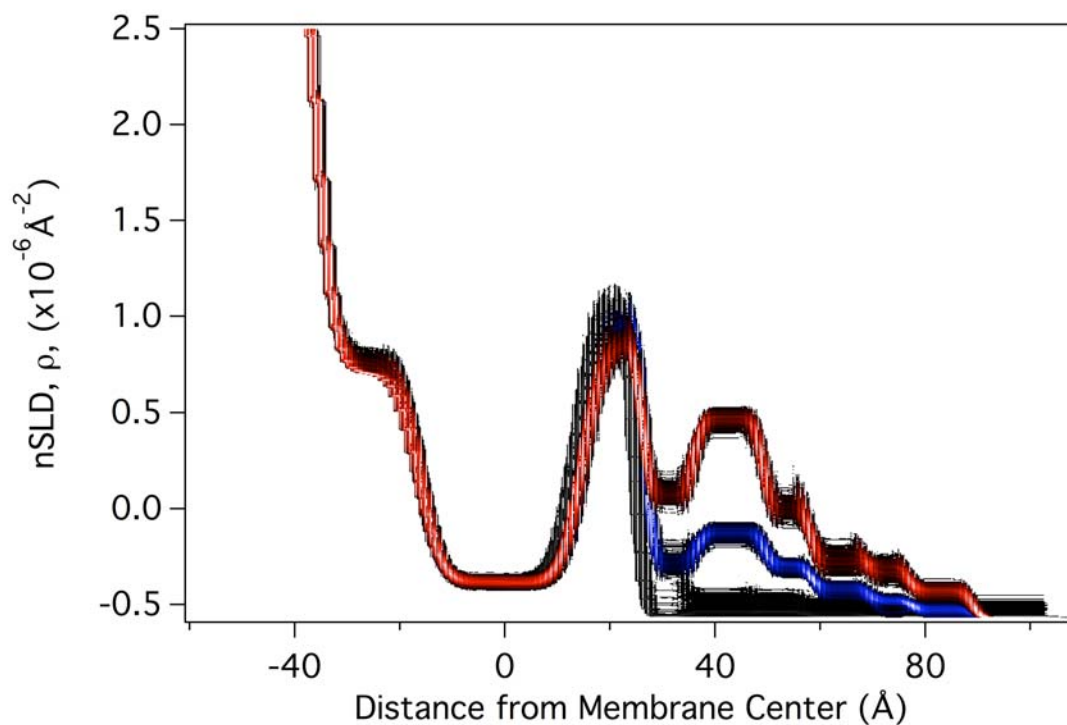


**Figure S4:** Free-form SLD profiles resulting from simultaneous fitting of the reflectivity data in Fig. S3. The neat bilayer (black), and tBLM with 1  $\mu\text{mol/L}$  MA (blue) and 10  $\mu\text{mol/L}$  MA (red) were all fitted with shared parameters for each isotopic contrast. Although they were not coupled in the fit, the profiles at 1 and 10  $\mu\text{mol/L}$  MA retain the same general structure in the region attributed to the protein contribution to the SLD, suggesting that MA binds to the interface in a monomolecular layer in which the protein attains a specific conformation and orientation.

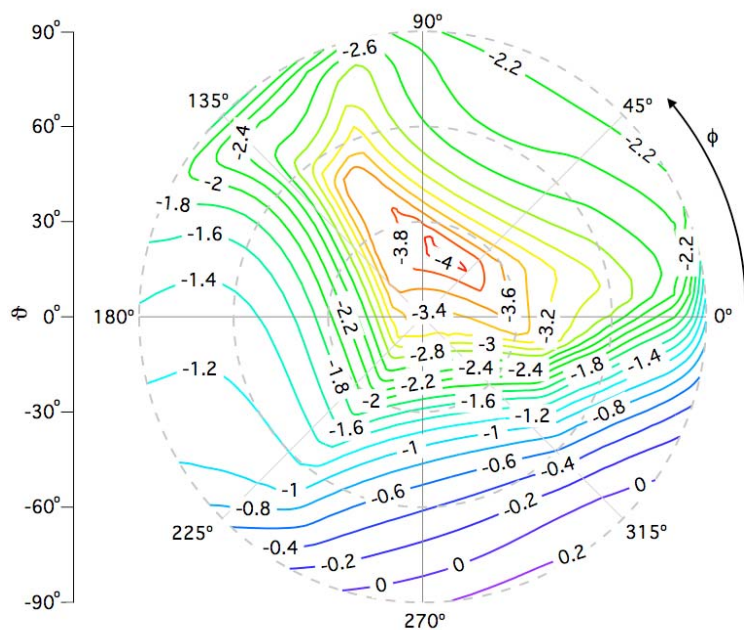


**Figure S5.** Electrostatic interaction of the  $-myrMA$  domain with a charged membrane surface at different orientations ( $\vartheta$ ,  $\phi$ ). Gouy-Chapman theory was used to estimate the binding energy (given in eV) using a Debye length,  $1/\kappa = 13.7 \text{ \AA}$ , consistent with the concentration of monovalent salt,  $c_{NaCl} = 50 \text{ mM}$ , used in the NR experiments.

## References.

1. Commercial materials, equipment, and instruments identified in this manuscript does not imply a recommendation or endorsement by the National Institute of Standards and Technology.
2. McLaughlin, S. 1989. The electrostatic properties of membranes. *Annu. Rev. Biophys. Biophys. Chem.* 18:113-136.
3. MacKerell, A., D. Bashford, M. Bellott, R. Dunbrack, J. Evanseck, M. Field, S. Fischer, J. Gao, H. Guo, S. Ha, D. Joseph-McCarthy, L. Kuchnir, K. Kuczera, F. Lau, C. Mattos, S. Michnick, T. Ngo, D. Nguyen, B. Prodhom, W. Reiher, B. Roux, M. Schlenkrich, J. Smith, R. Stote, J. Straub, M. Watanabe, J. Wiorkiewicz-Kuczera, D. Yin, and M. Karplus. 1998. All-atom empirical potential for molecular modeling and dynamics studies of proteins. *J. Phys. Chem. B* 102:3586-3616.
4. Dalton, A. K., D. Ako-Adjei, P. S. Murray, D. Murray, and V. M. Vogt. 2007. Electrostatic interactions drive membrane association of the human immunodeficiency virus type 1 Gag MA domain. *J. Virol.* 81:6434-6445.
5. Dalton, A. K., P. S. Murray, D. Murray, and V. M. Vogt. 2005. Biochemical characterization of rous sarcoma virus MA protein interaction with membranes. *J. Virol.* 79:6227-6238.

6. Murray, P. S., Z. Li, J. Wang, C. L. Tang, B. Honig, and D. Murray. 2005. Retroviral matrix domains share electrostatic homology: models for membrane binding function throughout the viral life cycle. *Structure* 13:1521-1531.